

### Electronic and Steric Control of Regioselectivities in Rh(I)-Catalyzed (5 + 2) Cycloadditions: Experiment and Theory

Peng Liu,<sup>†</sup> Lauren E. Sirois,<sup>‡</sup> Paul Ha-Yeon Cheong,<sup>†,§</sup> Zhi-Xiang Yu,<sup>†,⊥</sup>  
Ingo V. Hartung,<sup>‡,¶</sup> Heiko Rieck,<sup>‡,□</sup> Paul A. Wender,<sup>\*,‡</sup> and K. N. Houk<sup>\*,†</sup>

Department of Chemistry and Biochemistry, University of California, Los Angeles,  
California 90095-1569, and Department of Chemistry, Stanford University,  
Stanford, California 94305-5080

Received April 17, 2010; E-mail: wenderp@stanford.edu; houk@chem.ucla.edu

**Abstract:** The first studies on the regioselectivity of Rh(I)-catalyzed (5 + 2) cycloadditions between vinylcyclopropanes (VCPs) and alkynes have been conducted experimentally and analyzed using density functional theory (DFT). The previously unexplored regiochemical consequences for this catalytic, intermolecular cycloaddition were determined by studying the reactions of several substituted VCPs with a range of unsymmetrical alkynes. Experimental trends were identified, and a predictive model was established. VCPs with terminal substitution on the alkene reacted with high regioselectivity (>20:1), as predicted by a theoretical model in which bulkier alkyne substituents prefer to be distal to the forming C–C bond to avoid steric repulsions. VCPs with substitution at the internal position of the alkene reacted with variable regioselectivity (ranging from >20:1 to a reversed 1:2.3), suggesting a refined model in which electron-withdrawing substituents on the alkyne decrease or reverse sterically controlled selectivity by stabilizing the transition state in which the substituent is proximal to the forming C–C bond.

#### Introduction

A preeminent goal of synthesis is the generation of structural complexity and functional value with step economy.<sup>1</sup> As evident from the impact of the Diels–Alder (4 + 2) reaction in synthesis, cycloadditions are especially powerful in this regard. They proceed in one step with the convergent assembly of simple components into a new ring or ring system with multiple stereocenters. Studies on metal-mediated cycloadditions for the synthesis of medium-sized rings represent a particularly important area of research, given the number of structurally novel and biologically potent targets that incorporate such rings. Although the introduction of methods for the synthesis of seven-membered rings still lags behind that for smaller rings (particularly for catalytic, fully intermolecular variants), noteworthy progress has been made.<sup>2</sup> In 1995, we reported the first examples of metal-catalyzed (5 + 2) cycloadditions between vinylcyclopropanes (VCPs) and  $\pi$ -systems,<sup>3</sup> a homologue of the Diels–Alder cycloaddition that provides a general and effective route to

cycloheptene derivatives.<sup>4</sup> Figuring as a new strategy-level reaction in several syntheses,<sup>5</sup> the intramolecular version of this reaction provides a single cycloadduct regioisomer with respect to insertion of the two-carbon component due to the structural constraints of the tether between it and the VCP. Thus far, however, the steric and electronic factors influencing the regiochemistry of the unconstrained intermolecular process (which is currently limited to catalysis by rhodium) have not

<sup>†</sup> University of California.

<sup>‡</sup> Stanford University.

<sup>§</sup> Present address: Department of Chemistry, Oregon State University, Corvallis, OR 97331.

<sup>⊥</sup> Present address: College of Chemistry, Peking University, Beijing 100871, P.R. China.

<sup>¶</sup> Present address: Global Drug Discovery, Lead Generation & Optimization, Bayer-Schering Pharma AG, 42096 Wuppertal, Germany.

<sup>□</sup> Present address: PM Project Management, Bayer CropScience AG, 40789 Monheim am Rhein, Germany.

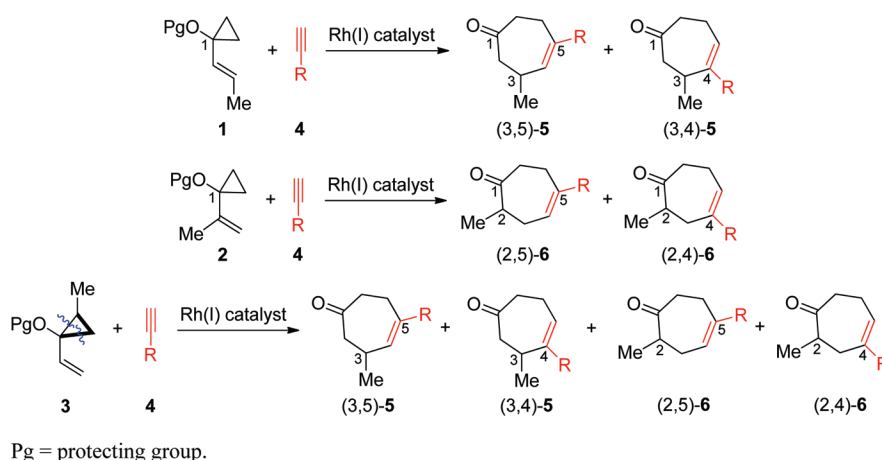
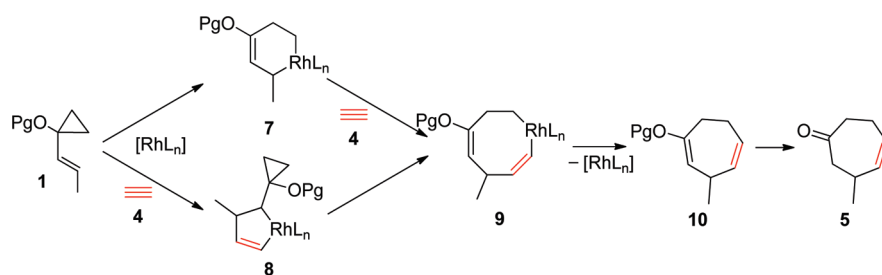
(1) (a) Wender, P. A.; Handy, S. T.; Wright, D. L. *Chem. Ind.* **1997**, 765–769. (b) Wender, P. A.; Croatt, M. P.; Witulski, B. *Tetrahedron* **2006**, 62, 7505–7511, references therein. (c) Wender, P. A.; Verma, V. A.; Paxton, T. J.; Pillow, T. H. *Acc. Chem. Res.* **2008**, 41, 40–49. (d) Wender, P. A.; Miller, B. L. *Nature* **2009**, 460, 197–201.

(2) (a) Yet, L. *Chem. Rev.* **2000**, 100, 2963–3007. (b) Battiste, M. A.; Pelphrey, P. M.; Wright, D. L. *Chem.—Eur. J.* **2006**, 12, 3438–3447. (c) Wender, P. A.; Croatt, M. P.; Deschamps, N. M. In *Comprehensive Organometallic Chemistry III*; Crabtree, R. H., Mingos, D. M. P., Eds.; Elsevier: Oxford, 2007; Vol. 10, pp 603–648. (d) Butenschön, H. *Angew. Chem., Int. Ed.* **2008**, 47, 5287–5290.

(3) For the first report, see: Wender, P. A.; Takahashi, H.; Witulski, B. *J. Am. Chem. Soc.* **1995**, 117, 4720–4721.

(4) For intermolecular reactions involving alkynes, see: (a) Wender, P. A.; Rieck, H.; Fuji, M. *J. Am. Chem. Soc.* **1998**, 120, 10976–10977. (b) Wender, P. A.; Dyckman, A. J.; Husfeld, C. O.; Scanio, M. J. C. *Org. Lett.* **2000**, 2, 1609–1611. (c) Wender, P. A.; Barzilay, C. M.; Dyckman, A. J. *J. Am. Chem. Soc.* **2001**, 123, 179–180. (d) Wender, P. A.; Gamber, G. G.; Scanio, M. J. C. *Angew. Chem., Int. Ed.* **2001**, 40, 3895–3897. (e) Wender, P. A.; Stemmler, R. T.; Sirois, L. E. *J. Am. Chem. Soc.* **2010**, 132, 2532–2533. (f) Wender, P. A.; Sirois, L. E.; Stemmler, R. T.; Williams, T. J. *Org. Lett.* **2010**, 12, 1604–1607. For intermolecular reactions involving allenes, see: (g) Wegner, H. A.; de Meijere, A.; Wender, P. A. *J. Am. Chem. Soc.* **2005**, 127, 6530–6531.

(5) For uses of the intramolecular (5 + 2) reaction in synthesis, see: (a) Wender, P. A.; Fuji, M.; Husfeld, C. O.; Love, J. A. *Org. Lett.* **1999**, 1, 137–139. (b) Wender, P. A.; Zhang, L. *Org. Lett.* **2000**, 2, 2323–2326. (c) Wender, P. A.; Bi, F. C.; Brodney, M. A.; Gosselin, F. *Org. Lett.* **2001**, 3, 2105–2108. (d) Ashfeld, B. L.; Martin, S. F. *Tetrahedron* **2006**, 62, 10497–10506. (e) Trost, B. M.; Hu, Y.; Horne, D. B. *J. Am. Chem. Soc.* **2007**, 129, 11781–11790. (f) Trost, B. M.; Waser, J.; Meyer, A. *J. Am. Chem. Soc.* **2008**, 130, 16424–16434.

**Scheme 1.** Possible Regioisomers in (5 + 2) Cycloadditions between Substituted VCPs and Terminal Alkynes**Scheme 2.** Possible Mechanistic Pathways for the Rhodium-Catalyzed (5 + 2) Cycloaddition

been addressed.<sup>6</sup> Substituted VCPs such as **1** and unsymmetrically substituted alkynes could lead to two regioisomeric products (Scheme 1). Cycloadduct (3,4)-**5** would have groups positioned vicinally as is observed with tethered substituents in the intramolecular process, whereas cycloadduct (3,5)-**5** would have a substitution pattern complementary to the intramolecular process. VCP **2** also offers a possible route to regioisomeric adducts but now having a different substitution pattern relative to that of VCP **1**. In the reaction of VCP **3**, a more complex scenario could unfold as four regioisomeric products are possible. While critical to the predictable use of the intermolecular process for accessing more substituted, complex synthetic targets, the regiochemistry of Rh(I)-catalyzed intermolecular (5 + 2) cycloadditions has not previously been explored experimentally or analyzed theoretically.

There are two general mechanisms proposed for the rhodium-catalyzed (5 + 2) cycloaddition. One would proceed through initial formation of a metallacyclohexene followed by alkyne insertion and reductive elimination (Scheme 2). A second would involve initial formation of a metallacyclopentene followed by cleavage of the cyclopropane (ring expansion) and reductive elimination. We have previously reported on the mechanism for the reactions of VCPs with simple acetylene, analyzing data from density functional theory (DFT) calculations.<sup>7</sup> According to the theoretical studies, the metallacyclohexene mechanism is preferred, and the rate-determining step is the alkyne insertion

to form an eight-membered metallacycle intermediate. The regioselectivities of oxidative addition or migratory insertion of alkenes and alkynes to form metallacycles have been investigated theoretically for a subset of other organometallic reactions.<sup>8</sup> For example, oxidative additions of bis(olefin)metal complexes in general favor the product in which electron-withdrawing substituents are positioned  $\alpha$  to the metal to maximize coefficients on the  $\beta$ -carbon, thereby facilitating C–C bond formation. However, reactions involving alkynes usually do not follow this trend, and in many cases the regioselectivities are dominated by steric effects. At present neither the regioselectivity preference for the metal-catalyzed intermolecular (5 + 2) cycloaddition nor its magnitude is known. Thus, we sought to establish the experimental regioselectivities for a standard set of alkynes and VCPs and to analyze these data using DFT calculations. Regioselectivity is a key factor in the predictive use of a new reaction, and its exploration becomes part of the touchstone for synthetic applications of the method.<sup>9</sup> The widespread use of the Diels–Alder<sup>10</sup> reaction in synthesis, for

(6) For studies involving regiochemical aspects of the rhodium- and ruthenium-catalyzed intramolecular processes, see: (a) Wender, P. A.; Dyckman, A. J. *Org. Lett.* **1999**, *1*, 2089–2092. (b) Wender, P. A.; Dyckman, A. J.; Husfeld, C. O.; Kadereit, D.; Love, J. A.; Rieck, H. *J. Am. Chem. Soc.* **1999**, *121*, 10442–10443. (c) Trost, B. M.; Shen, H. C. *Org. Lett.* **2000**, *2*, 2523–2525. (d) Trost, B. M.; Shen, H. C.; Horne, D. B.; Toste, F. D.; Steinmetz, B. G.; Koradin, C. *Chem.–Eur. J.* **2005**, *11*, 2577–2590.

(7) (a) Yu, Z.-X.; Wender, P. A.; Houk, K. N. *J. Am. Chem. Soc.* **2004**, *126*, 9154–9155. (b) Yu, Z.-X.; Cheong, P. H.-Y.; Liu, P.; Legault, C. Y.; Wender, P. A.; Houk, K. N. *J. Am. Chem. Soc.* **2008**, *130*, 2378–2379. (c) Liu, P.; Cheong, P. H.-Y.; Yu, Z.-X.; Wender, P. A.; Houk, K. N. *Angew. Chem., Int. Ed.* **2008**, *47*, 3939–3941.

(8) For examples of related theoretical studies on the regioselectivity of metal-catalyzed reactions with substituted alkynes, see: (a) Stockis, A.; Hoffmann, R. *J. Am. Chem. Soc.* **1980**, *102*, 2952–2962. (b) Wakatsuki, Y.; Nomura, O.; Kitaura, K.; Morokuma, K.; Yamazaki, H. *J. Am. Chem. Soc.* **1983**, *105*, 1907–1912. (c) Dahy, A. A.; Koga, N. *Bull. Chem. Soc. Jpn.* **2005**, *78*, 781–791. (d) Yamamoto, Y.; Kinpara, K.; Saigoku, F.; Takagishi, H.; Okuda, S.; Nishiyama, H.; Itoh, K. *J. Am. Chem. Soc.* **2005**, *127*, 605–613. (e) Liu, P.; Jordan, R. W.; Kibbee, S. P.; Goddard, J. D.; Tam, W. *J. Org. Chem.* **2006**, *71*, 3793–3803. For related insights, see: (f) Dalton, D. M.; Oberg, K. M.; Yu, R. T.; Lee, E. E.; Perreault, S.; Oinen, M. E.; Pease, M. L.; Malik, G.; Rovis, T. *J. Am. Chem. Soc.* **2009**, *131*, 15717–15728.

**Table 1.** (5 + 2) Cycloadditions of VCP **1a** and Terminal Alkynes<sup>a</sup>

entry	alkyne	R	time (h)	TFE <sup>b</sup> (%)	product	yield <sup>c</sup> (%)	(3,5)-5:(3,4)-5 <sup>d</sup>
1	<b>4a</b>	<i>n</i> -Pr	4.25	25	<b>5a</b>	78	>20:1
2	<b>4c</b>	CM <sub>2</sub> OH	22	—	<b>5c</b>	69	>20:1
3	<b>4d</b>	TMS	18	5	<b>5d</b>	74	>20:1
4	<b>4e</b>	CO <sub>2</sub> Me	8.25	5	<b>5e</b>	90	>20:1
5	<b>4f</b>	COMe	23	5	<b>5f</b>	77	>20:1
6	<b>4h</b>	Ph	4.75	25	<b>5h</b>	84	>20:1

<sup>a</sup> Conditions: 1.2–1.5 equiv of alkyne **4**, 5 mol % [Rh(CO)<sub>2</sub>Cl]<sub>2</sub>, DCE or TFE/DCE (0.1 M), 40 °C; 1% HCl/EtOH. DCE = 1,2-dichloroethane; TFE = 2,2,2-trifluoroethanol. <sup>b</sup> Volume percent. <sup>c</sup> Combined isolated yield. <sup>d</sup> Ratio determined by <sup>1</sup>H NMR.

example, is largely due to the body of knowledge that has been accumulated regarding predictable regio- and stereoselective outcomes. We report herein the first experimental study of the regioselectivities of these synthetically useful (5 + 2) reactions and a theoretical study that predicts the trends observed experimentally and explains the origins of the steric and electronic factors that control regioselectivity.

## Results and Discussion

The (5 + 2) cycloadditions were performed under the conditions outlined in Table 1. Significantly, the reactions of terminally substituted VCP **1a** with terminal alkynes resulted in exclusive formation of 3,5-disubstituted cycloheptenones (3,5)-**5**.<sup>11</sup> This dramatic preference was observed for both electron-rich and -poor alkynes (entries 1–3 and 4–5, respectively). From a synthetic viewpoint, the resulting (3,5)-substitution pattern preference complements the regioselectivity of the intramolecular process, which provides vicinally positioned substituents with complete selectivity. Despite the increased steric encumbrance of VCP **1a** relative to that of an unsubstituted VCP, cycloadducts (3,5)-**5** were isolated as the ketone products in good to excellent yields following mildly acidic workup. In many cases the addition of 2,2,2-trifluoroethanol (TFE) as a cosolvent in 1,2-dichloroethane (DCE) allowed for shorter reaction times and improved yields without affecting the regioselective outcome.<sup>12</sup>

For reactions of internally substituted VCP **2a**, the formation of 5-substituted adducts (2,5)-**6**, now having a different substitution pattern (2,5 for VCP **2a** vs 3,5 for VCP **1a**), were again

**Table 2.** (5 + 2) Cycloadditions of VCP **2a** and Terminal Alkynes<sup>a</sup>

entry	alkyne	R	time (h)	TFE <sup>b</sup> (%)	product(s)	yield <sup>c</sup> (%)	(2,5)-6:(2,4)-6 <sup>d</sup>
1	<b>4a</b>	<i>n</i> -Pr	48	5	<b>6a</b>	76	7.1:1
2	<b>4b</b>	CH <sub>2</sub> OH	6	—	<b>6b</b>	77	3.1:1
3	<b>4c</b>	CM <sub>2</sub> OH	5	—	<b>6c</b>	73	>20:1
4	<b>4d</b>	TMS	18	5	<b>6d</b>	85	>20:1
5	<b>4e</b>	CO <sub>2</sub> Me	4.25	5	<b>6e</b>	84	3.0:1
6	<b>4f</b>	COMe	5	—	<b>6f</b>	84	1:1.7
7	<b>4f</b>	COMe	2.75	5	<b>6f</b>	91	1:1.9
8 <sup>e</sup>	<b>4f</b>	COMe	11.5	5	<b>6f</b>	84	1:2.3
9	<b>4g</b>	CO- <i>p</i> -CF <sub>3</sub> -Ph	8	—	<b>6g</b>	66	2.4:1
10	<b>4g</b>	CO- <i>p</i> -CF <sub>3</sub> -Ph	4.5	5	<b>6g</b>	82	2.2:1
11	<b>4h</b>	Ph	7	5	<b>6h</b>	78	7.7:1

<sup>a</sup> Conditions: 1.2–1.5 equiv of alkyne **4**, 5 mol % [Rh(CO)<sub>2</sub>Cl]<sub>2</sub>, DCE or TFE/DCE (0.1 M), 40 °C; 1% HCl/EtOH. <sup>b</sup> Volume percent. <sup>c</sup> Combined isolated yield. <sup>d</sup> Ratio determined by <sup>1</sup>H NMR. <sup>e</sup> 1 mol % [Rh(CO)<sub>2</sub>Cl]<sub>2</sub>.

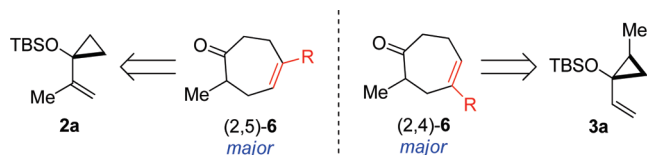
favored, but in many cases to a lesser extent (Table 2). The use of larger or electron-rich alkyne substituents resulted in high selectivities (>20:1) and good yields (entries 3–4). For alkynes with electron-withdrawing substituents, calculations (vide infra) predict that the regioselectivity should be attenuated, if not reversed, by electronic effects. This expectation was borne out experimentally with electron-poor alkynes affording cycloadducts with reduced (entries 5, 9–10) and even reversed regioselectivities (entries 6–8) in good combined yields.<sup>13</sup> Catalyst loading can be lowered to 1 mol %, although a longer reaction time is required (entry 8). As observed for VCP **1a**, addition of TFE cosolvent improved the reaction times and yields with negligible change in regioselectivity.

For studies of the (5 + 2) reaction and its regioselectivity, VCP **3a** represents an interesting case, as four regioisomeric products could be formed with an unsymmetrical alkyne (see also Scheme 5 and discussion below). When an additional substituent is present on the cyclopropane ring, oxidative cyclization with rhodium can proceed with cleavage of either the more- or less-substituted cyclopropyl bond. According to our mechanistic proposal (vide infra), cleavage of the more substituted cyclopropane bond would give rise to (3,5)-**5** and (3,4)-**5** products, whereas cleavage of the less substituted bond would afford (2,5)-**6** and (2,4)-**6** cycloadducts. If the substituent on the cyclopropane ring is a methyl group, these are collectively the same products as for (5 + 2) reactions of VCPs **1a** and **2a**. The results of representative (5 + 2) reactions of VCP **3a** with ethynyltrimethylsilane, methyl propiolate, and 3-buten-2-one are given in Table 3.

For the cycloaddition of VCP **3a** and ethynyltrimethylsilane (entry 1), only one observable product was formed, the 4-substituted adduct (2,4)-**6d** with the methyl group from the VCP  $\alpha$  to the ketone, representing cleavage of the less

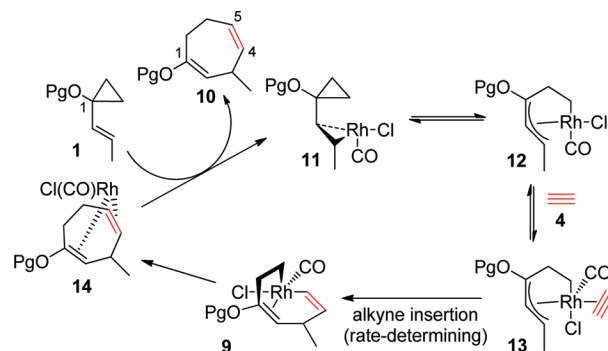
- (9) For recent representative examples of regiochemical consequences in other Rh(I)-catalyzed intermolecular cycloadditions (e.g., (2 + 2 + 2), (3 + 2 + 2), and (4 + 2 + 2) reactions) involving alkynes, see: (a) Friedman, R. K.; Rovis, T. *J. Am. Chem. Soc.* **2009**, *131*, 10775–10782, and references therein. (b) Evans, P. A.; Inglesby, P. A. *J. Am. Chem. Soc.* **2008**, *130*, 12838–12839. (c) Tanaka, K. *Synlett* **2007**, 1977–1993, and references therein. (d) Evans, P. A.; Lai, K. W.; Sawyer, J. R. *J. Am. Chem. Soc.* **2005**, *127*, 12466–12467. (e) Gilbertson, S. R.; DeBoef, B. *J. Am. Chem. Soc.* **2002**, *124*, 8784–8785. (f) Murakami, M.; Ubukata, M.; Itami, K.; Ito, Y. *Angew. Chem., Int. Ed.* **1998**, *37*, 2248–2250.
- (10) Review: Nicolaou, K. C.; Snyder, S. A.; Montagnon, T.; Vassilikogiannakis, G. *Angew. Chem., Int. Ed.* **2002**, *41*, 1668–1698, and references therein.
- (11) Minor proximal cycloadduct (3,4)-**5f** was observed in trace amount by GC–MS; for all other reactions of VCP **1a**, a single cycloadduct peak was observed in GC–MS analysis of the crude reaction mixture and was later determined to correspond to the product indicated.

- (12) For a review of the use of fluorinated alcohols in catalysis, see: (a) Shuklov, I. A.; Dubrovina, N. V.; Börner, A. *Synthesis* **2007**, 2925–2943. For similar effects, see: (b) Reference 3. (c) Reference 4c. (d) Wender, P. A.; Croatt, M. P.; Deschamps, N. M. *Angew. Chem., Int. Ed.* **2006**, *45*, 2459–2462. (e) Saito, A.; Ono, T.; Hanzawa, Y. *J. Org. Chem.* **2006**, *71*, 6437–6443.
- (13) For a related observation, see: Wender, P. A.; Christy, J. P. *J. Am. Chem. Soc.* **2006**, *128*, 5354–5355.

**Scheme 3.** VCPs **2a** and **3a** Provide Access to Regiochemically Complementary Cycloadducts

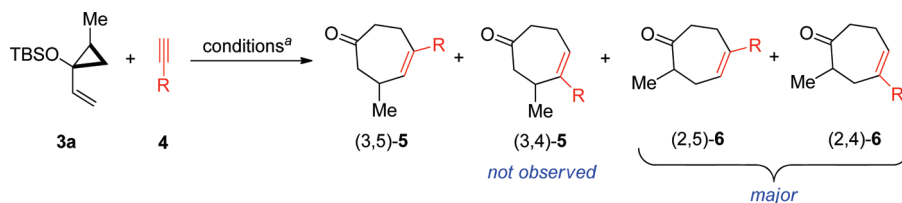
substituted cyclopropane bond.<sup>14</sup> The 4-substituted product (2,4)-**6e** was also favored for the reaction of methyl propiolate, in a ~3:1 ratio over 5-substituted adduct (2,5)-**6e**. These results have important ramifications for synthetic applications as they suggest that, for a given alkyne, one could selectively produce either the (2,5)- or the (2,4)-substituted regioisomer by judicious selection of the appropriate VCP (**2a** or **3a**, respectively, Scheme 3). VCP **3a** provides access to the regiochemically complementary products of reactions of VCP **2a**, with 4-substituted adducts favored for the former to a similar degree that 5-substituted adducts are favored for the latter. Interestingly, the (5 + 2) cycloaddition of methyl propiolate also provided a small amount of product (3,5)-**5e**, resulting from cleavage of the more substituted cyclopropyl bond. A significant amount of (3,5)-**5f** (similarly resulting from cleavage of the more substituted cyclopropyl bond) was also produced from reaction of VCP **3a** with 3-butyne-2-one. In accordance with the reversal of regioselectivity versus reactions of VCP **2a**, in this case 5-substituted adduct (2,5)-**6f** was formed preferentially over 4-substituted adduct (2,4)-**6f** in a 2.5:1 ratio (Table 3, entry 3 versus Table 2, entry 7). In no case were products (3,4)-**5** observed at the completion of the cycloaddition. This, too, is synthetically significant as that type of substitution is alternatively available with complete selectivity through the intramolecular (5 + 2) reaction.

To analyze these trends and to uncover the steric and electronic effects at play, calculations with density functional theory (B3LYP/SDD-6-31G\* with CPCM solvation model) were performed. Previous theoretical studies<sup>7</sup> revealed that rhodium-catalyzed intermolecular (5 + 2) cycloadditions likely occur via the catalytic cycle shown in Scheme 4. The rate-determining step is the alkyne insertion to form the eight-membered rhodacycle intermediate **9**. Thus, cycloadditions with unsymmetrically substituted alkynes could lead to two regioisomeric products based upon the orientation of the alkyne during migratory insertion. Accordingly, the regioselectivity is determined by the energy difference between these *distal* and *proximal* alkyne insertion transition states ( $\Delta\Delta G^\ddagger(\text{prox-dis})$ , vide infra). *Distal* is defined here as alkyne substituent R positioned

**Scheme 4.** Catalytic Cycle for Rh(I)-Catalyzed (5 + 2) Cycloadditions

away from the forming C–C bond in the  $2\pi$  insertion transition state; *proximal* is defined as R oriented toward the forming C–C bond (and away from the metal center). The activation free energies of *distal*- and *proximal*-transition states **TS1**, **TS2**, and **TS3** for cycloadditions between VCP **1b**, **2b**, or **3b** and terminal alkynes are given in Tables 4, 5, and 6, respectively. To reduce computational time, a smaller methyl group (Pg = Me) was used as a proxy for the silyl group (Pg = TBS) on the C-1 oxygen of the VCPs, since 1-methoxy and 1-siloxy VCPs are predicted to have similar regioselectivities.<sup>15</sup> Computational results reflect experimental trends for the vast majority of examples studied; indeed, disagreements between the *in vitro* and *in silico* product ratios are generally observed only for cases in which the energy differences are computed to be quite small ( $\leq 1$  kcal/mol). Thus, these findings begin to suggest a predictive model for the regiochemical outcomes of these reactions.

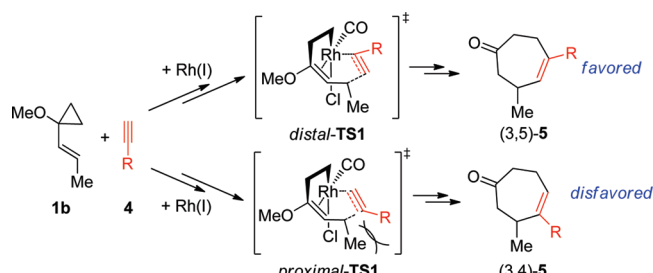
According to the theoretical models, in the rate- and regiochemistry-determining alkyne insertion transition states, the alkyne is in the same plane as rhodium and the two carbons formerly comprising the vinyl group of the VCP (Figure 1). Two possible steric interactions might arise in the alkyne insertion transition state when a bulky group is present on the alkyne: repulsions between the alkyne substituent R and the VCP terminus in the *proximal*-**TS** and repulsions between R and the catalyst in the *distal*-**TS**. For reactions with all VCPs, the repulsion between alkyne substituent R and the VCP-derived fragment is stronger than that between R and the metal center or ligands, as indicated by spatial and bond length analysis. For reactions of VCP **1b**, significant repulsions are observed between the alkyne substituent R and the methyl group on the terminal position of the VCP metallacycle in *proximal*-**TS1**. Thus, formation of (3,5)-substituted products is strongly favored for the cycloadditions of VCP **1b** with all alkynes (Table 4). To

**Table 3.** (5 + 2) Cycloadditions of VCP **3a** and Terminal Alkynes<sup>a</sup>

entry	alkyne	R	time (h)	product(s)	yield <sup>b</sup> (%)	(3,5)-5:(3,4)-5:(2,5)-6:(2,4)-6 <sup>c</sup>
1	<b>4d</b>	TMS	18	<b>6d</b>	87	0:0:1:>20
2	<b>4e</b>	CO <sub>2</sub> Me	31	<b>5e/6e</b>	69	1:0:2.1:6.4
3	<b>4f</b>	COMe	10	<b>5f/6f</b>	86	1.7:0:2.5:1

<sup>a</sup> Conditions: 1.2–1.3 equiv of alkyne **4**, 5 mol % [Rh(CO)<sub>2</sub>Cl]<sub>2</sub>, TFE (5 vol %) in DCE (0.1 M), 40 °C; 1% HCl/EtOH. <sup>b</sup> Combined isolated yield. <sup>c</sup> Ratio determined by <sup>1</sup>H NMR.



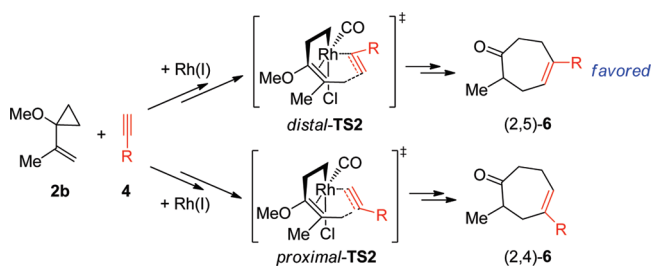
**Table 4.** B3LYP/SDD-6-31G\*/CPCM(DCE) Free Energies of Activation for (5 + 2) Cycloadditions between VCP **1b** and Terminal Alkynes


entry	alkyne	R	$\Delta G^\ddagger(\text{TS1})^{a,b}$		$\Delta\Delta G^\ddagger(\text{prox-dis})^b$	predicted ratio <sup>c</sup> (3,5)-5:(3,4)-5
			distal-	proximal-		
1	<b>4i</b>	H	7.0	7.0	—	—
2	<b>4j</b>	Me	10.9	16.1	5.1	>20:1
3	<b>4a</b>	<i>n</i> -Pr	12.1	17.5	5.4	>20:1 <sup>d</sup>
4	<b>4k</b>	<i>t</i> -Bu	13.9	25.7	11.8	>20:1
5	<b>4b</b>	CH <sub>2</sub> OH	6.4	13.5	7.1	>20:1
6	<b>4c</b>	CMe <sub>2</sub> OH	8.0	19.4	11.4	>20:1 <sup>d</sup>
7	<b>4d</b>	TMS	7.1	15.1	8.0	>20:1 <sup>d</sup>
8	<b>4e</b>	CO <sub>2</sub> Me	9.1	11.7	2.5	>20:1 <sup>d</sup>
9	<b>4f</b>	COMe	9.1	10.6	1.4	11:1 <sup>d</sup>
10	<b>4g</b>	CO- <i>p</i> -CF <sub>3</sub> -Ph	10.4	12.5	2.1	>20:1
11	<b>4l</b>	CH=O	7.3	8.3	1.0	5.3:1
12	<b>4m</b>	CN	7.5	9.8	2.3	>20:1
13	<b>4h</b>	Ph	14.0	19.6	5.6	>20:1 <sup>d</sup>
14	<b>4n</b>	NH <sub>2</sub>	7.6	13.6	6.1	>20:1

<sup>a</sup> Relative to the Rh(CO)Cl–VCP  $\pi$ -complex. <sup>b</sup> Energies in kcal/mol. <sup>c</sup> Calculated ratio at 298 K. <sup>d</sup> See Table 1 for ratio observed experimentally.

illustrate this effect, the transition state structures for the reaction between VCP **1b** and propyne **4j** ( $R = \text{Me}$ ) are shown in Figure 1. The *distal* transition state, *distal-TS1j*, is strongly favored by 5.1 kcal/mol. Due to larger steric repulsions, the forming C–C bond length in *proximal-TS1j* is 0.06 Å longer than in *distal-TS1j*. For cycloadditions involving other alkyl-substituted alkynes, the *distal* pathway preferences correlate with the steric bulk of the alkyl groups (entries 2–4, Table 4). Cycloadditions of internally substituted VCP **2b** exhibit a slightly diminished preference for the *distal* pathway, due to the reduced steric bulk of the VCP terminus. For example, the reaction between pentyne **4a** ( $R = n\text{-Pr}$ ) and VCP **1b** is highly *distal*-selective ( $\Delta\Delta G^\ddagger = 5.4$  kcal/mol), whereas the analogous reaction involving VCP **2b** is less so ( $\Delta\Delta G^\ddagger = 1.3$  kcal/mol, experimentally 1.2 kcal/mol or 7.1:1).

While steric effects appear to govern the regioselectivity of many of these reactions, the combined experimental and theoretical results indicate that electronic effects related to the alkyne substituent also have a significant influence on the degree and even the sense of regioselectivity. Electron-donating substituents reinforce the steric preference for *distal* alkyne orientation in **TS1** and **TS2**. For example, the small, but powerfully electron-donating amino substituent of alkyne **4n** ( $R = \text{NH}_2$ ) is predicted to yield the 5-substituted product exclusively for both VCPs **1b** and **2b** (entry 14, Table 4 and entry 14, Table 5). In

**Table 5.** B3LYP/SDD-6-31G\*/CPCM(DCE) Free Energies of Activation for (5 + 2) Cycloadditions between VCP **2b** and Terminal Alkynes


entry	alkyne	R	$\Delta G^\ddagger(\text{TS2})^{a,b}$		$\Delta\Delta G^\ddagger(\text{prox-dis})^b$	predicted ratio <sup>c</sup> (2,5)-6:(2,4)-6
			distal-	proximal-		
1	<b>4i</b>	H	7.8	7.8	—	—
2	<b>4j</b>	Me	11.9	12.8	0.9	4.9:1
3	<b>4a</b>	<i>n</i> -Pr	12.8	14.1	1.3	8.5:1 <sup>d</sup>
4	<b>4k</b>	<i>t</i> -Bu	14.9	18.8	3.8	>20:1
5	<b>4b</b>	CH <sub>2</sub> OH	7.3	10.3	2.9	>20:1 <sup>d</sup>
6	<b>4c</b>	CMe <sub>2</sub> OH	8.5	12.9	4.3	>20:1 <sup>d</sup>
7	<b>4d</b>	TMS	14.6	16.9	2.2	>20:1 <sup>d</sup>
8	<b>4e</b>	CO <sub>2</sub> Me	10.2	10.3	0.1	1.2:1 <sup>d</sup>
9	<b>4f</b>	COMe	10.9	8.7	−2.2	1:>20 <sup>d</sup>
10	<b>4g</b>	CO- <i>p</i> -CF <sub>3</sub> -Ph	11.7	11.5	−0.2	1:1.3 <sup>d</sup>
11	<b>4l</b>	CH=O	8.6	6.8	−1.8	1:20
12	<b>4m</b>	CN	8.5	9.6	1.1	6.4:1
13	<b>4h</b>	Ph	15.4	17.6	2.2	>20:1 <sup>d</sup>
14	<b>4n</b>	NH <sub>2</sub>	8.5	11.9	3.4	>20:1

<sup>a</sup> Relative to the Rh(CO)Cl–VCP  $\pi$ -complex. <sup>b</sup> Energies in kcal/mol. <sup>c</sup> Calculated ratio at 298 K. <sup>d</sup> See Table 2 for ratio observed experimentally.

contrast, electron-withdrawing groups on the alkyne stabilize *proximal-TS1* and *-TS2*, the pathways leading to 4-substituted products. This orientation allows the largest coefficient of the alkyne  $\pi^*$  orbital to interact with the metal, thus enhancing back-donation of electron density from the filled rhodium  $d_{xy}$  orbital (Figure 2). The resultant stability manifests itself in lower activation barriers for *proximal-TS* for electron-withdrawing substituents as compared to alkyl or phenyl alkyne substituents. For the cycloadditions of VCP **2b** and alkynes with small and strongly electron-withdrawing groups, such as ketones or aldehydes (entries 9 and 11, Table 5<sup>16</sup>), these electronic effects dominate over steric repulsion and reverse the regioselectivity to favor the 4-substituted product (Figure 2).

As briefly discussed above, when additional substitution is present on the cyclopropane (as in VCP **3**), the ring can open in two ways during oxidative cyclization, with cleavage of either the more- or less-substituted bond. For each of the resulting metallacyclohexenes, the subsequent alkyne insertion step can then proceed with the alkyne in either of two different orientations (as for VCPs **1** and **2**), leading to 4-substituted and 5-substituted products for each (Scheme 5). If the cyclopropyl substituent is a methyl group, the four possible regioisomeric cycloadducts are the same as the possible products from (5 + 2) reactions of VCPs **1** and **2** with terminal alkynes, i.e., (3,4)-**5**, (3,5)-**5**, (2,4)-**6**, and (2,5)-**6**. However, different trends of regioselectivity are observed, since the alkyne insertion orientations leading to either 4-substituted or 5-substituted products are reversed relative to those in **TS1** and **TS2**. *Distal-TS3-a*

- (14) For examples of intramolecular (5 + 2) reactions featuring cyclopropyl substitution and studies of catalyst and stereochemical influence on cyclopropyl ring cleavage, see references 5 and 6.
- (15) 1-Methoxy VCPs ( $\text{Pg} = \text{Me}$ ) were surrogates for 1-silyloxy VCPs ( $\text{Pg} = \text{TBS}$ ) in the calculations due to their similar regioselectivities. Reaction of 1-TMSO-VCP **2** and propynal (**4l**) is computed to favor the *proximal* pathway by 1.6 kcal/mol, similar to the 1.8 kcal/mol *proximal* preference for the 1-MeO-VCP **2b** (Table 5, entry 11).

- (16) A very small *proximal* preference is predicted for alkyne **4g** (Table 5, entry 10). This corresponds to the low regioselectivity observed experimentally for alkyne **4g** (Table 2, entries 9 and 10), in which, however, the *distal* product (2,5)-**6g** is slightly favored.

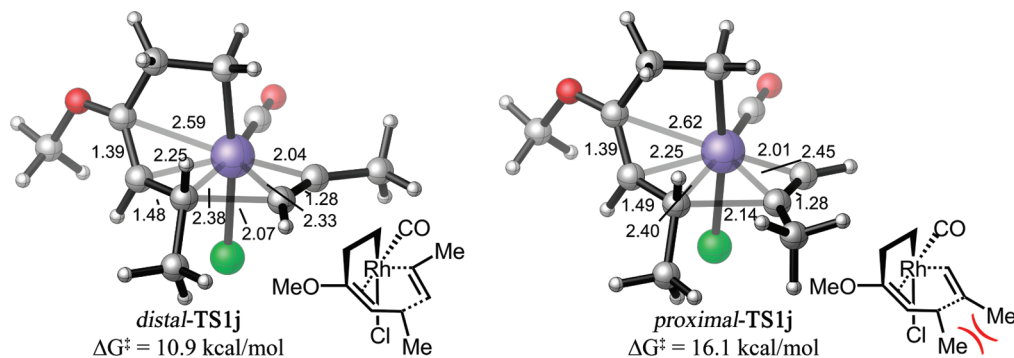
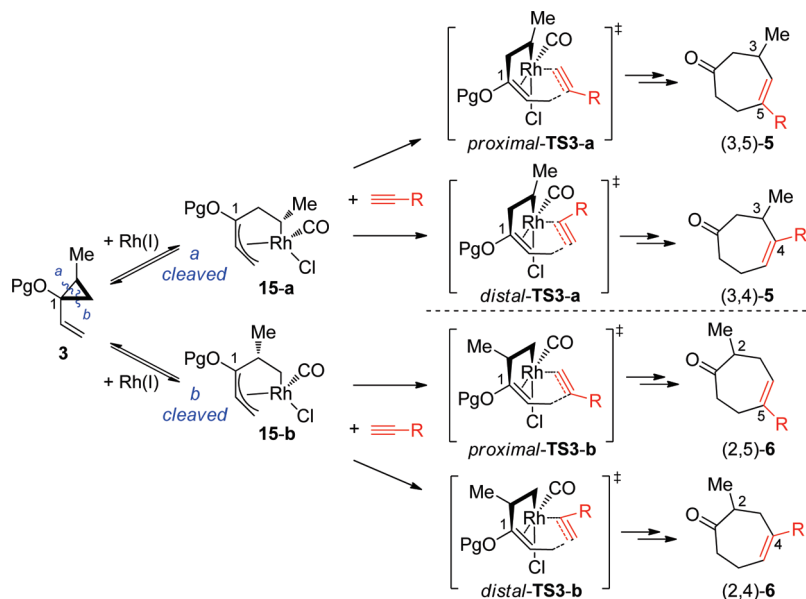


**Figure 1.** Optimized structures of the alkyne insertion transition states *distal*- and *proximal*-TS1j for the cycloaddition of VCP **1b** with propyne (**4j**).

**Scheme 5.** Possible Regioisomeric Pathways for Rh(I)-Catalyzed (5 + 2) Cycloadditions of VCP **3<sup>a</sup>**



<sup>a</sup> Single enantiomers of **15-a**, **15-b**, **TS3-a**, and **TS3-b** are depicted for clarity.

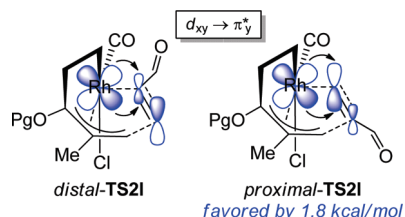


**Figure 2.** Stabilizing back-donation from the rhodium  $d_{xy}$  orbital to  $\pi^*_y$  of the alkyne is largest in the *proximal* transition state (illustrated here for **TS2** involving VCP **2b** and alkyne **4l**).

and **-TS3-b**, in which the alkyne substituent **R** is *distal* to the forming C–C bond, ultimately lead to 4-substituted products, while *proximal*-**TS3-a** and **-TS3-b**, in which **R** is *proximal* to the forming C–C bond, ultimately lead to 5-substituted products (Scheme 5).

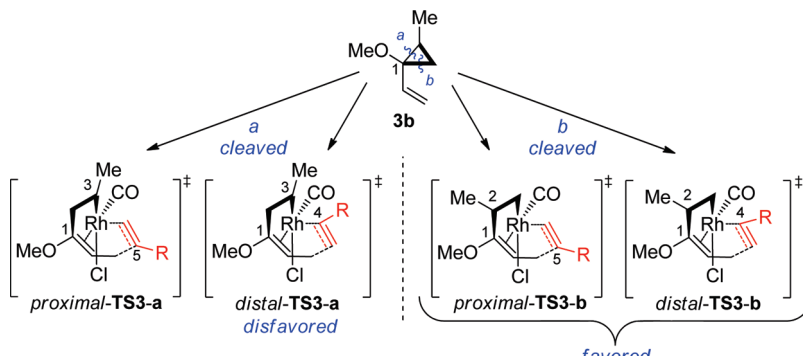
Cleavage of either the more- or less-substituted cyclopropyl C–C bond of VCP **3b** (Pg = Me) is predicted to be very fast. The activation barriers for cleavage of the more substituted (bond *a* cleaved) and less substituted (bond *b* cleaved) cyclopropyl C–C bonds are only 2.1 and 0.4 kcal/mol, respectively, with respect to the Rh(CO)Cl–VCP  $\pi$  complex. These barriers are much lower than those of any of the subsequent alkyne insertion steps possible. Thus, in

this scenario, the cleavage of cyclopropyl C–C bonds is reversible and the two metallacyclic intermediates **15-a** and **15-b** are in equilibrium with each other. Previous theoretical and experimental studies on rhodium(I)-catalyzed (5 + 2) reactions also suggest that steps prior to alkyne insertion in the catalytic cycle are reversible.<sup>17</sup> Insertion of alkyne to intermediates **15-a** and **15-b** leads to stable eight-membered metallacycles (see intermediate **9**, for example, Scheme 4). This step is irreversible (see Supporting Information for details). Thus, alkyne insertion (**TS3**) is the regioselectivity-determining step.<sup>18</sup> Under these Curtin–Hammett-like conditions,<sup>19</sup> the distribution of cycloadduct formation is determined by the energy differences among the alkyne insertion transition states in the four regioisomeric pathways. The calculated activation energies for the four pathways of the reactions of VCP **3b** and several alkynes are given in Table 6.

(17) See references 6b and 7, for example.

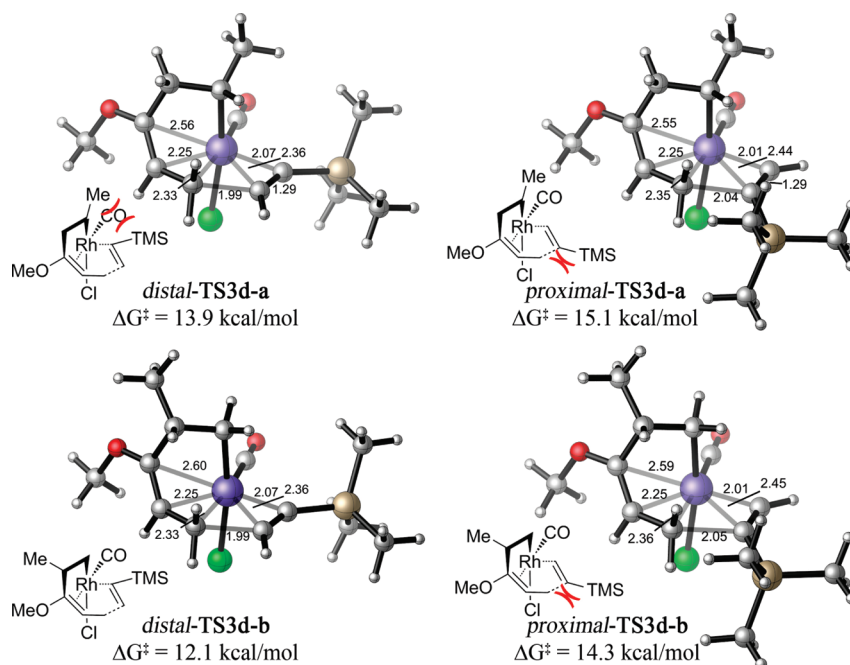
(18) For all pathways except *distal-a*, alkyne insertion is also the rate-determining step. For pathway *distal-a*, subsequent reductive elimination requires slightly higher activation energies than alkyne insertion. Thus, both alkyne insertion and reductive elimination are the slow steps in the catalytic cycle for pathway *distal-a*. See Supporting Information for details.

(19) (a) Seeman, J. I. *Chem. Rev.* **1983**, 83, 83–134. (b) Seeman, J. I. *J. Chem. Educ.* **1986**, 63, 42–48.

**Table 6.** B3LYP/SDD-6-31G\*/CPCM(DCE) Free Energies of Activation of the Alkyne Insertion Transition States for (5 + 2) Cycloadditions between VCP **3b** and Terminal Alkynes


entry	alkyne	R	$\Delta G^\ddagger(\text{TS3})^{a,b}$			
			proximal-TS3-a	distal-TS3-a	proximal-TS3-b	distal-TS3-b
1	<b>4i</b>	H	6.3	6.3	5.5	5.5
2	<b>4j</b>	Me	11.8	10.9	10.9	10.0
3	<b>4d</b>	TMS	15.1	13.9	14.3	12.1
4	<b>4e</b>	CO <sub>2</sub> Me	9.0	8.9	8.8	8.1
5	<b>4f</b>	COMe	7.5	9.6	7.8	9.0
6	<b>4l</b>	CH=O	5.4	7.3	5.8	6.5

<sup>a</sup> Relative to the Rh(CO)Cl–VCP  $\pi$ -complex. <sup>b</sup> Energies in kcal/mol.

**Figure 3.** Optimized structures of the alkyne insertion transition states for the cycloaddition of VCP **3b** and alkyne **4d**.

The relative activation energies among the four possible alkyne insertion transition states of the reactions of VCP **3b** are influenced by several factors. As explained in the analysis for VCPs **1b** and **2b**, one can imagine steric repulsions related to the alkyne substituent and the forming C–C bond in the *proximal* transition states for VCP **3b**, as well as the energy-lowering electronic influence of strong backbonding from rhodium to the  $\pi^*$  orbital of the alkyne in these same *proximal* transition states when the substituent thereon is electron-withdrawing (see Figure 2). Moreover, for VCP **3b**, the *distal* transition states involving cleavage of the more substituted cyclopropyl bond (*distal-TS3-a*) are destabilized by potential repulsions between the methyl group on the

cyclopropyl ring and the R substituent on the alkyne. To exemplify these points graphically, the computed transition states for the reaction of VCP **3b** and alkyne **4d** (R = TMS) are illustrated in Figure 3.

For example, due to steric repulsions associated with the forming C–C bond, bulky alkyne substituents such as TMS orient *distal* to the forming C–C bond in the lower-energy alkyne insertion transition states (*distal-TS3-a* and *-TS3-b*). Furthermore, the steric interaction of an especially bulky alkyne substituent such as TMS with the methyl group from cyclopropane results in a lower activation barrier for *distal-TS3-b* as compared to *distal-TS3-a*. Thus, in these cases, *distal-TS3-b* is the most favored pathway, leading to cy-

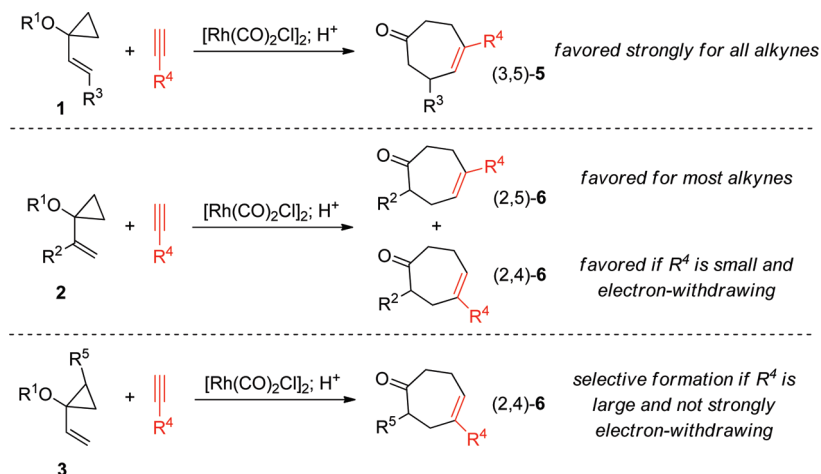


**Figure 4.** Summary of regiochemical outcomes for intermolecular (5 + 2) reactions of VCPs **1**, **2**, and **3** with terminal alkynes.

cloadducts (2,4)-**6** preferentially (entries 2 and 3, Table 6). Conversely, for alkynes with small and strongly electron-withdrawing groups such as formyl or acyl, stabilizing  $d \rightarrow \pi^*$  backbonding interactions are maximized when R is *proximal* to the forming C–C bond (*proximal-TS3*). Thus, when this R group is small, both pathways leading to 5-substituted products (*proximal-TS3-a* and *-TS3-b*) are computed to be lower in energy (entries 5 and 6, Table 6), and because cleavage of either the more- or less-substituted cyclopropyl bonds is reversible, several products are expected. For alkyne **4e** ( $R = \text{CO}_2\text{Me}$ ), all four pathways are computed to have similar activation energies due to competing steric and electronic effects.

## Conclusions

The sense and magnitude of the regioselectivity preferences for Rh(I)-catalyzed (5 + 2) cycloadditions of substituted VCPs and substituted alkynes have been established experimentally and analyzed theoretically (see Figure 4 for a summary of outcomes). The regioselectivity is controlled by the steric encumbrance of the alkyne substituent, moderated or reversed in select cases by electronic effects. Bulky or electron-rich alkyne substituents are postulated to orient *distal* to the forming C–C bond during alkyne insertion to avoid steric repulsions, leading to preferential formation of (3,5)- and (2,5)-disubstituted cycloadducts **5** and **6**, respectively, for VCPs of type **1** and **2**, over the (3,4)- and (2,4)-disubstituted regioisomers. Electron-withdrawing substituents on the alkyne decrease or reverse this selectivity by stabilizing the transition state in which the substituent is *proximal* to the forming C–C bond in the alkyne insertion transition states. The regiochemistry-determining alkyne insertion transition states involving VCPs such as **3** are subject to these same steric and electronic influences while providing synthetically complementary products. These studies provide the experimental and mechanistic foundation for understanding and predicting regioselectivities in the Rh-catalyzed intermolecular (5 + 2) cycloaddition and related processes in synthesis. Additionally, when considered with the intramolecular (5 + 2) reactions, this work provides the basis for

selective access to (3,4)-, (3,5)-, (2,5)-, and (2,4)-substituted cycloheptenones.

## Experimental Section

**General Procedure for (5 + 2) Cycloadditions.** In an oven-dried, argon-purged glass test tube fitted with a rubber septum,  $[\text{Rh}(\text{CO})_2\text{Cl}]_2$  catalyst (0.025 mmol, 9.7 mg) was dissolved in freshly distilled DCE (2.5 mL) at room temperature to form a homogeneous yellow solution. In a separate oven-dried, nitrogen-flushed glass vial fitted with a rubber septum, vinylcyclopropane (0.500 mmol, 106 mg) was dissolved in DCE (1.0 mL). Under an inert atmosphere, this colorless solution was transferred with rinsing (1.5 mL DCE) via syringe to the vessel containing the stirring rhodium catalyst solution. Argon was bubbled through a needle into the resulting yellow solution for five minutes before addition of an alkyne (0.60–0.75 mmol) in a single portion via syringe. Solid alkynes were dissolved in 1.0 mL of the total DCE volume to be used and transferred under an inert atmosphere. The reaction vessel was then immediately lowered into a preheated 40 °C oil bath and allowed to stir under positive pressure of argon for the indicated time. Upon consumption of the VCP (as indicated by TLC analysis), the reaction solution was cooled to room temperature and treated with 0.1 mL of a 1% HCl/EtOH solution. After hydrolysis of enol ether cycloadduct(s) (generally 5–20 min), the reaction solution was passed through a short pad of silica gel with  $\text{Et}_2\text{O}$  eluent and concentrated *in vacuo* to a brown oil. Following initial GC–MS and  $^1\text{H}$  NMR analysis, the crude product(s) were purified via silica gel flash column chromatography (EtOAc/pentane or  $\text{Et}_2\text{O}$ /petroleum ether eluent). For reactions producing multiple regioisomers, (5 + 2) cycloadducts were collected together following chromatography, and a combined isolated yield was reported. When feasible, further chromatography furnished analytically pure samples of each regioisomer for spectroscopic analysis. When TFE was used, it was added to the stirring mixture of VCP and  $[\text{Rh}(\text{CO})_2\text{Cl}]_2$  in DCE (reduced volume) prior to bubbling of argon through the reaction solution. Full experimental details and characterization data can be found in the accompanying Supporting Information.

**Theoretical Calculations.** Geometry optimizations, frequencies, and solvation energy calculations were performed with the B3LYP functional implemented in Gaussian 03.<sup>20</sup> The Stuttgart/Dresden effective core potential<sup>21</sup> was used on rhodium, and the 6-31G(d) basis set was employed for other atoms. All

(20) Frisch, M. J.; et al. *Gaussian 03*, Rev. D.01; Gaussian, Inc.: Wallingford, CT, 2004.



reported free energies involve zero-point vibrational energy corrections, thermal corrections to Gibbs free energy at 298 K, and solvation free energy corrections computed by singlet point CPCM<sup>22</sup> calculations on gas-phase optimized geometries. Parameters for the solvent used in experiments, 1,2-dichloroethane ( $\epsilon = 10.125$ ), were used in the CPCM calculations. The molecular cavities were built up using the United Atom Topological Model (UAHF), which was reported to be more accurate than cavity models such as UFF, Pauling, or Bondi in

calculating solvation free energies using CPCM.<sup>23</sup> Figures 1 and 3 were prepared using CYLView.<sup>24</sup>

**Acknowledgment.** We thank the National Science Foundation (CHE-0548209, CHE-0450638, and CHE-0131944), the NSF Graduate Research Fellowship (L.E.S.), Deutsche Forschungsgemeinschaft (H.R.), and Deutscher Akademischer Austausch Dienst (I.V.H.) for financial support. The Vincent Coates Foundation Mass Spectrometry Laboratory at Stanford University and TeraGrid resources provided by NCSA are acknowledged for mass spectra and computational facilities.

**Supporting Information Available:** Complete experimental details and characterization data for cycloadducts and preparation of VCPs. Complete reference 20 and optimized geometries and energies of all computed species. This material is available free of charge via the Internet at <http://pubs.acs.org>.

- (21) Andrae, D.; Haussermann, U.; Dolg, M.; Stoll, H.; Preuss, H. *Theor. Chim. Acta* **1990**, *77*, 123–141.
- (22) (a) Barone, V.; Cossi, M. *J. Phys. Chem. A* **1998**, *102*, 1995–2001. (b) Cossi, M.; Rega, N.; Scalmani, G.; Barone, V. *J. Comput. Chem.* **2003**, *24*, 669–681.
- (23) (a) Barone, V.; Cossi, M.; Tomasi, J. *J. Chem. Phys.* **1997**, *107*, 3210–3221. (b) Houk, K. N.; Tahano, Y. *J. Chem. Theory Comput.* **2005**, *1*, 70–77. (c) Gao, D. Q.; Svoronos, P.; Wong, P. K.; Maddalena, D.; Hwang, J.; Walker, H. *J. Phys. Chem. A* **2005**, *109*, 10776–10785. (d) Yu, A.; Liu, Y.; Wang, Y. *Chem. Phys. Lett.* **2007**, *436*, 276–279.
- (24) Legault, C. Y. *CYLview*, 1.0b; Université de Sherbrooke: Québec, Montreal, Canada, 2009; <http://www.cylview.org>.

JA103253D